Suppression of 19S proteasome subunits marks emergence of an altered cell state in diverse cancers

Citation: Tsvetkov, Peter et al. "Suppression of 19S Proteasome Subunits Marks Emergence of an Altered Cell State in Diverse Cancers." Proceedings of the National Academy of Sciences 114, 2 (Janaury 2017): 382–387 © 2017 National Academy of Sciences

As Published: http://dx.doi.org/10.1073/pnas.1619067114

Publisher: National Academy of Sciences (U.S.)

Persistent URL: http://hdl.handle.net/1721.1/111198

Version: Final published version: final published article, as it appeared in a journal, conference proceedings, or other formally published context

Suppression of 19S proteasome subunits marks emergence of an altered cell state in diverse cancers

Peter Tsvetkov[a,1], Ethan Sokol[a,b], Dexter Jin[a,b], Zarina Brune[a], Prathapan Thiru[a], Mahmoud Ghandi[c], Levi A. Garraway[c,d,e], Piyush B. Gupta[a,b,f,g], Sandro Santagata[h], Luke Whitesell[a], and Susan Lindquist[a,b,i,2]

[a]Whitehead Institute for Biomedical Research, Cambridge, MA 02142; [b]Department of Biology, Massachusetts Institute of Technology, Cambridge, MA 02139; [c]Broad Institute, Cambridge, MA 02142; [d]Dana-Farber Cancer Institute, Harvard Medical School, Boston, MA 02215; [e]Department of Medicine, Brigham and Women's Hospital, Harvard Medical School, Boston, MA 02115; [f]Koch Institute for Integrative Cancer Research, Cambridge, MA 02139; [g]Harvard Stem Cell Institute, Cambridge, MA 02138; [h]Department of Pathology, Brigham and Women's Hospital, Harvard Medical School, Boston, MA 02115; and [i]Howard Hughes Medical Institute, Cambridge, MA 02139

Edited by Carol Prives, Columbia University, New York, NY, and approved December 5, 2016 (received for review November 22, 2016)

The use of proteasome inhibitors to target cancer's dependence on altered protein homeostasis has been greatly limited by intrinsic and acquired resistance. Analyzing data from thousands of cancer lines and tumors, we find that those with suppressed expression of one or more 19S proteasome subunits show intrinsic proteasome inhibitor resistance. Moreover, such proteasome subunit suppression is associated with poor outcome in myeloma patients, where proteasome inhibitors are a mainstay of treatment. Beyond conferring resistance to proteasome inhibitors, proteasome subunit suppression also serves as a sentinel of a more global remodeling of the transcriptome. This remodeling produces a distinct gene signature and new vulnerabilities to the proapoptotic drug, ABT-263. This frequent, naturally arising imbalance in 19S regulatory complex composition is achieved through a variety of mechanisms, including DNA methylation, and marks the emergence of a heritably altered and therapeutically relevant state in diverse cancers.

drug resistance | epigenetic gene regulation | apoptosis | EMT | bortezomib

Cells rely on the proteasome machinery to mediate protein turnover and maintain protein homeostasis (1–3). Upon oncogenic transformation, a myriad of proteotoxic stresses that tax the cellular machinery responsible for protein homeostasis are introduced (2, 4). These pressures cause cancer cells to rely heavily on enhanced proteasome function (2, 5–8). This dependency can be exploited using natural and synthetic compounds that inhibit, with exquisite potency and selectivity, the catalytic function of the 20S proteasome (9, 10). Indeed, these compounds are highly effective at inhibiting the growth of a wide variety of cancer cell lines in culture. Unfortunately, their clinical utility has been surprisingly limited, with therapeutic benefits commonly observed for only a few types of cancer (9, 10).

The limited role for proteasome inhibitors as clinical chemotherapeutics can be attributed to biological processes that promote intrinsic and acquired resistance. For example, cell culture models of acquired resistance often accumulate mutations in the catalytic subunits of the 20S proteasome (11, 12). In terms of clinical relevance, however, such mutations have yet to be detected in clinical samples (13). Additional mechanisms of resistance include alteration of specific cellular pathways such as constitutive activation of NF-κB (14), activation of the chaperone machinery (15, 16), or alterations in the EGFR/JAK1/STAT3 pathway (17).

To further explore and identify the cellular mechanisms of resistance developed in the presence of distinct proteasome inhibitors, our group and others recently applied genome-wide genetic screens to various cell-line models (18, 19). In all models examined, experimentally reducing the expression of one of the many different subunits composing the 19S regulatory complex increases resistance to inhibitors of the proteasome's catalytic core (18, 19) and may show clinical relevance in multiple myeloma patients (18). These data suggested that transient, nonmutational mechanisms may play a key role in the ability of cancer cells to withstand proteasome inhibition. In this work we examine if such a mechanism is implemented by different cancers.

Results

Sharply Reduced Expression of One 19S Proteasome Complex Subunit Occurs Frequently Across Diverse Cancer Cell Lines. We first characterized relative mRNA expression levels for all genes that encode proteasome subunits using the Genomics of Drug Sensitivity in Cancer (GDSC) database (20). As expected, across 789 cancer cell lines, the average expression level of 20S subunits was highly correlated with the average expression level of 19S subunits (Fig. 1*A*). However, in some cell lines, the expression of a specific 19S subunit was much lower than the average expression of that subunit across all cell lines. To quantify this phenomenon for each cell line in the GDSC and the Cancer Cell Line Encyclopedia (CCLE) datasets, we calculated the SD from the mean of every 19S subunit in every cell line. Each cell line was then assigned a sigma score that is indicative of the greatest deviation from the mean of any one 19S subunit in that cell line. Thus, a sigma score of 3 indicates a cell line in which the mRNA expression of at least one subunit of the 19S proteasome complex was reduced by 3 SDs from the mean mRNA level of that particular subunit across all cell lines. A sigma score of 2 indicates a reduction in the mRNA of 2 SDs, and so on.

In 59 cancer cell lines, the mRNA level of at least one 19S subunit was 3 or more SDs (3σ) from the mean for that subunit

Significance

In previous work, we used genome-wide screening to uncover a counterintuitive mechanism by which cells can acquire resistance to inhibitors of the proteasome's catalytic core through experimentally induced imbalances in the composition of its regulatory particle. However, in many cases, mechanisms uncovered in vitro for acquired resistance often do not translate to the context of actual clinical cancers. Here, we show that this mechanism is actually deployed spontaneously and naturally in diverse human cancer lines and is associated not only with increased resistance to proteasome inhibitors both in vitro and in the clinic but also is symptomatic of a much more broadly altered state with a unique gene signature and drug targetable vulnerabilities.

Author contributions: P. Tsvetkov designed research; P.B.G., L.W., and S.L. provided scientific supervision; P. Tsvetkov and Z.B. performed research; M.G. and L.A.G. contributed new reagents/analytic tools; P. Tsvetkov, E.S., D.J., P. Thiru, M.G., and P.B.G. analyzed data; and P. Tsvetkov, S.S., L.W., and S.L. wrote the paper.

Conflict of interest statement: L.A.G. is a consultant for Foundation Medicine, Novartis, Boehringer Ingelheim, and Third Rock; an equity holder in Foundation Medicine; and a member of the Scientific Advisory Board at Warp Drive. L.A.G. receives sponsored research support from Novartis, Astellas, BMS, and Merck.

This article is a PNAS Direct Submission.

[1]To whom correspondence should be addressed. Email: petert@wi.mit.edu.

[2]Deceased October 27, 2016.

This article contains supporting information online at www.pnas.org/lookup/suppl/doi:10.1073/pnas.1619067114/-/DCSupplemental.

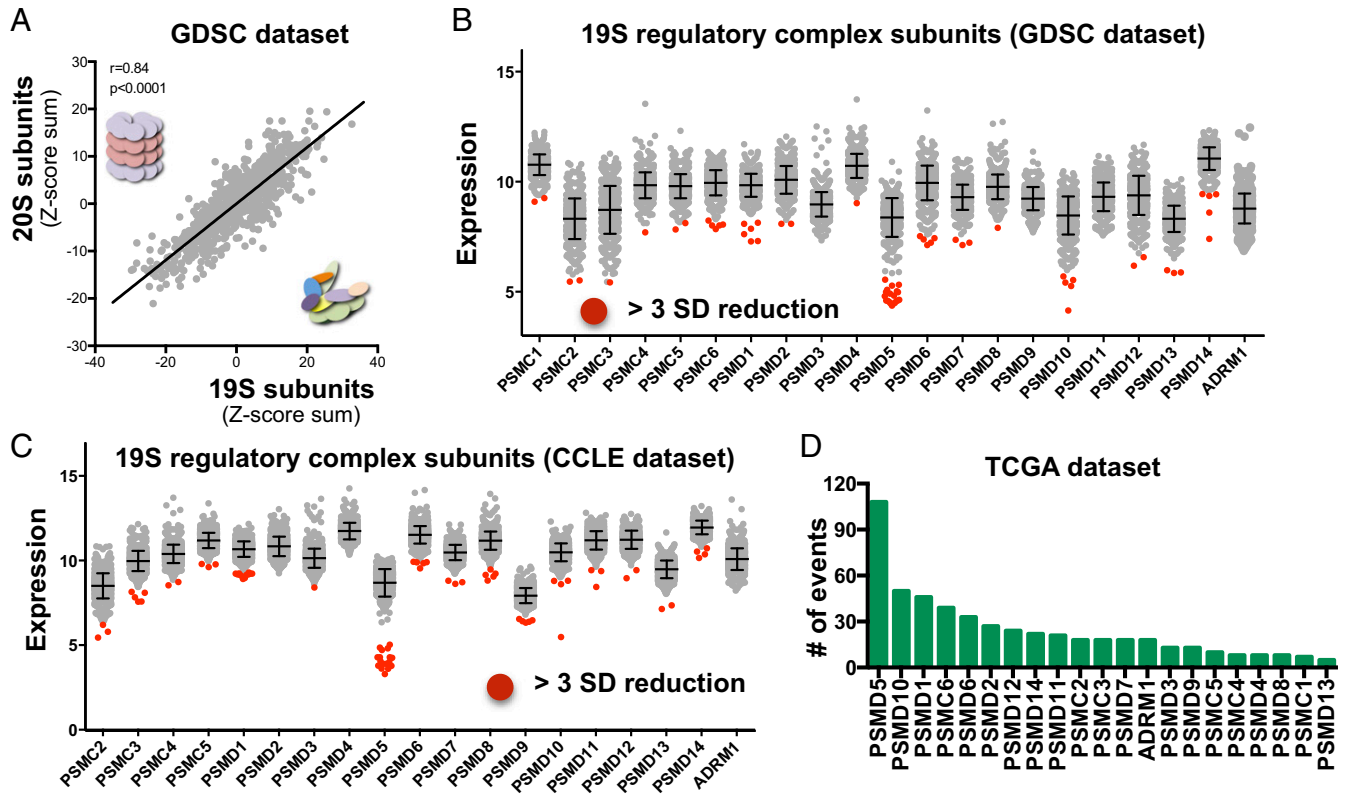

Fig. 1. Reduced expression of a single 19S proteasome complex subunit occurs naturally in many cancer cells. (*A*) The overall expression of all 26S proteasome subunits is tightly correlated. The correlation between the z-score sum of expression of 20S proteasome subunits versus the 19S proteasome subunits is plotted across 789 cancer cell lines taken from the GDSC dataset. Spearman correlation: $r = 0.84$ ($P < 0.0001$). (*B* and *C*) Representation of the expression levels for individual 19S subunits for each cancer cell line in the GDSC (*B*) and the CCLE datasets (*C*). Red dots indicate cells that exhibit reduced expression of a given subunit by more than 3 SDs from the mean (3σ). Each dot represents an individual cell line. (*D*) Analysis of primary tumor expression profiles taken from TCGA dataset. The value of each bar is the number of primary tumors exhibiting a 3σ drop in expression of at least one 19S subunit.

across all 789 cell lines in the GDSC dataset. For ease of reference, we designated these as "3σ lines" (Fig. 1*B*, red dots, and Dataset S1). We also analyzed the CCLE dataset that includes mRNA expression and DNA copy-number data for 990 cell lines. Of these, 6.3% were 3σ lines, a percentage similar to that in the GDSC dataset (Fig. 1*C*, red dots, and Dataset S1). To determine whether this strong deviation from the mean of 19S subunits could be explained by random variation in the expression of any 21 genes, we analyzed the frequency of 3σ lines in the GDSC and CCLE datasets for 1,000 random sets of 21 genes (Fig. S1 *A* and *B*). The frequency of 19S subunit 3σ cells was much higher than expected by chance in both the GDSC and CCLE datasets (*P* values = 1.1*e*-9 and 4.5*e*-12, respectively).

The particular 19S subunit gene that was suppressed varied among the 3σ cell lines (Fig. S1*C*). PSMD5 was the most commonly suppressed 19S proteasome subunit in both the GDSC and the CCLE cell-line datasets. Other frequently reduced subunits included PSMD1, PSMC6, PSMD10, PSMD14, and PSMD6. Overall, the mRNA expression of 19S subunits was reduced in cell lines representing a wide array of tumor types.

To investigate the frequency and patterns of 19S subunit mRNA suppression in resection specimens of human primary tumors, we further analyzed mRNA expression data from The Cancer Genome Atlas (TCGA). We examined the expression profiles of 8,557 primary tumors from 53 different cancer types. The frequency of tumors with a 3σ drop of at least one subunit of the 19S proteasome was 4.3% (Dataset S2). Moreover, this analysis of TCGA data showed that 3σ subunit reductions were present in tumors of diverse histology, amounting to 6–9% of some tumor types such as low-grade and high-grade gliomas, pheochromocytomas and paragangliomas, acute myeloid leukemias, renal cell carcinomas, and cutaneous melanomas (Fig. S1*D*).

Interestingly, as true for the GDSC and CCLE datasets, PSMD5 was the most commonly suppressed 19S subunit gene in human tumor resection samples (Fig. 1*D*). In addition, other 19S subunit genes that commonly showed changes in the GDSC and CCLE cell-line datasets such as *PSMD10*, *PSMD1*, *PSMC6*, and *PSMD6* were suppressed in tumor resection samples as well (Fig. 1*D*).

Reduced Expression of Any One of Many 19S Subunits Correlates Highly with Resistance to Proteasome Inhibitors. We next examined whether naturally occurring reduced expression of a 19S subunit correlated with the cells' ability to tolerate proteasome inhibition. We used 310 cell lines in the GDSC collection for which drug-sensitivity data were available and asked if our calculated sigma score correlated with the measured EC_{50} for two chemically distinct proteasome inhibitors, bortezomib and MG132 (Fig. 2*A* and Fig. S2*A*). Increases in the sigma score (i.e., reduced expression of a single 19S subunit) were highly correlated with increased resistance to both bortezomib and MG132. The correlation between sigma score and increased EC_{50} for proteasome inhibitors plateaued at approximately a sigma score of 3; cells with sigma scores of 4 or 5 did not have significantly higher EC_{50}'s than cells with sigma scores of 3 (Fig. 2*A* and Fig. S2*A*).

Comparisons of the mean EC_{50} for both bortezomib and MG132 between the control group of cell lines and the 3σ lines revealed a significantly higher EC_{50} in the 3σ group ($P < 0.0001$) (Fig. 2*B* and Fig. S2*B*). For bortezomib, the average natural log of the EC_{50} of the control group was −5.68, whereas the average natural log of the EC_{50} of the 3σ group was −3.56 (Fig. 2*B*). A similar sigma-score analysis for 20S proteasome subunit expression did not

MEDICAL SCIENCES

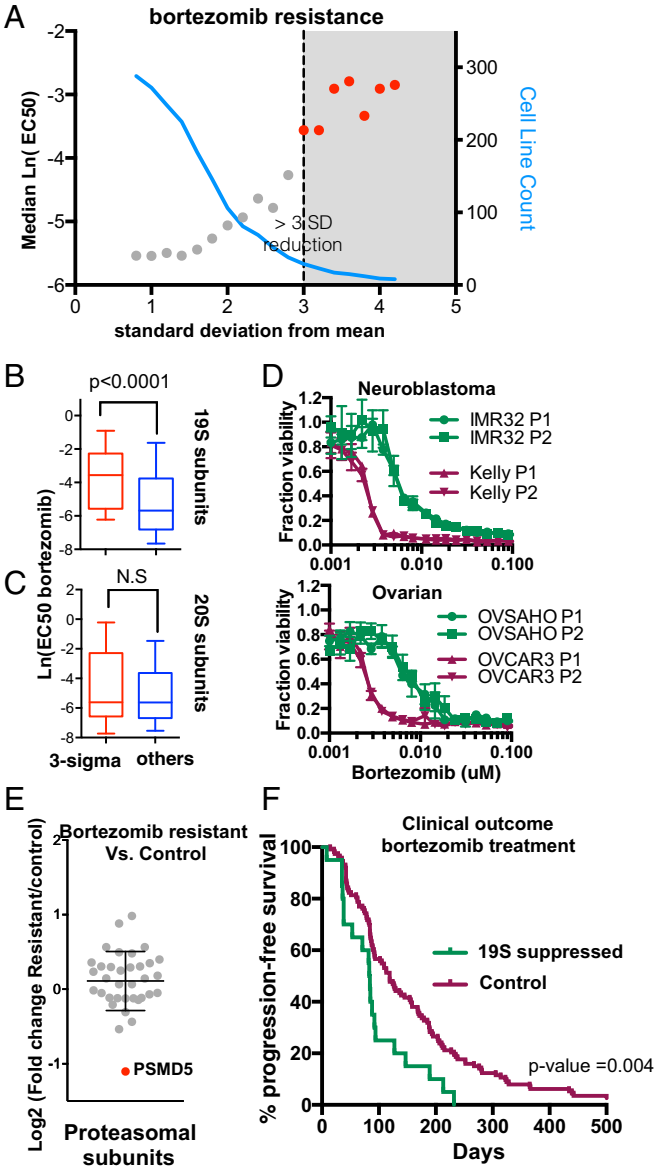

Fig. 2. Reduced expression of a single 19S proteasome complex subunit is associated with resistance to proteasome inhibitors. (*A*) The average bortezomib sensitivity of cells from the GDSC dataset is plotted against the suppression score of any one of their 19S subunits. Each point represents the median of the natural log EC_{50} for bortezomib (*y* axis) of all cells with at least one 19S proteasome subunit with reduced expression at the indicated SD from the mean (*x* axis). The blue line shows the number of cell lines for each SD—the higher the deviation, the fewer cell lines (right *y* axis). Cell lines that exhibit deviation of one 19S subunit by more than 3 SD (red dots) have higher EC_{50} for bortezomib. (*B* and *C*) Cell lines with 3σ reduction in mRNA expression of a 19S proteasome complex subunit (*B*) or a 20S proteasome subunit (*C*) were compared with all other cell lines (control) for sensitivity to bortezomib. The Mann–Whitney test was used to calculate a *P* value. (*D*) The viability of IMR32 and OVSAHO (reduced expression of 19S subunit) and Kelly and OVCAR3 (control) cell lines was examined following exposure to increasing concentrations of the proteasome inhibitor bortezomib. (*E*) The relative expression levels of all proteasome subunits were plotted as the log2 of the fold change in expression between the tumors derived from proteasome inhibitor-resistant cells or controls from a previously described model (21). (*F*) Time to relapse is plotted for patients that relapsed and were treated with bortezomib in phase 2 and phase 3 clinical trials of bortezomib (22). Patients are stratified by reduced expression of at least one subunit of the 19S proteasome complex vs. controls. *P* value was calculated by log-ranked (Mantel–Cox) test.

identify significant correlations with proteasome inhibitor EC_{50} (Fig. 2*C* and Fig. S2*B*), supporting the idea that the differential sensitivity to proteasome inhibitors is specifically dictated by reduced expression of subunits of the 19S proteasome complex.

We experimentally validated the effect of 19S subunit suppression on proteasome inhibitor sensitivity by examining two sets of cell lines derived from neuroblastoma and ovarian cancer, malignancies of very different histological origin. One line in each set had a natural suppression of one 19S subunit (IMR32, OVSAHO) whereas the other did not (Kelly, OVCAR3) (Dataset S1). The IMR32 neuroblastoma and OVSAHO ovarian cells have PSMD5 and PSMD9 subunit expression suppressed, respectively. As expected, cells with a naturally suppressed 19S subunit showed relative resistance to proteasome inhibition compared with corresponding lines of the same cancer type without subunit suppression (Fig. 2*D*).

Reduced 19S Subunit mRNA Expression Correlates with Inhibitor Resistance and Poor Outcome for Myeloma Patients Treated with Bortezomib. To determine whether the subunit-suppression mechanism of resistance that we identified has relevance in therapeutic settings, we analyzed gene-expression data from two sources: a laboratory-generated model of acquired resistance to proteasome inhibition (23) and patient tumor samples collected during clinical trials of bortezomib (22). The laboratory model involved the mantle cell lymphoma line Jeko-1 and a bortezomib-resistant variant (JBR cells) (23). The transcriptional profile of xenografts formed by these cell lines in mice (21) revealed a strong reduction in *PSMD5* mRNA levels in the tumors formed by the bortezomib-resistant JBR cells (Fig. 2*E*).

For patient-derived data, we mined correlative studies performed as part of key phase 2 and 3 clinical trials that were conducted in 2007 and established the efficacy of bortezomib in patients with recurrent multiple myeloma (22). Expression profiling data for pretreatment myeloma samples were available from these trials but posttreatment samples were not collected, precluding analysis of 19S subunit levels in the myeloma cells that emerged following bortezomib treatment and relapse. Strikingly, even in samples obtained before treatment, we found that reduced 19S subunit expression at baseline correlated with inferior disease control by bortezomib (Fig. 2*F*). Samples from 54 of 264 bortezomib-naive patients exhibited reduced expression of at least one of the 19S proteasome subunits. Of these 54 cases, 34 patients subsequently received bortezomib. These 34 patients exhibited a significantly shorter time to progression compared with the patients with myeloma that did not have relative suppression of 19S subunit expression ($P = 0.004$) (Fig. 2*F*). Notably, bortezomib treatment of patients with reduced expression of 19S proteasome subunit(s) showed no greater effectiveness than dexamethasone treatment in the control group. Nor did suppression of 19S subunit(s) induce a significant change in the efficacy of dexamethasone treatment (Fig. S2*C*).

Proteasome 19S Subunit Suppression Marks a Distinct Heritable State. To examine if the altered proteasome inhibitor sensitivity in the cells with 19S subunit suppression is part of a broader alteration to the cellular state, we created a rank-ordered list of gene-expression alterations in the 3σ cell lines. Analysis of CCLE and the GDSC datasets, comprising more than 1,000 cell lines, yielded very similar results. Cells with reduced expression of 19S subunits had a significant reduction in genes associated with several key oncogenic and signaling pathways. For example, the epithelial–mesenchymal transition (EMT) gene signature was significantly reduced (Fig. 3*A*, yellow, and Fig. S3 *A* and *B*). These cells also displayed a reduction in gene signatures related to EGF and TNF signaling (Fig. 3*A*, green, and Fig. S3*A*) and heat-shock–related genes (Fig. S3*C*). Such highly significant patterns of differential gene expression and gene-set enrichment are compelling, particularly given that they are derived from many diverse cancer cell lines.

Given the strong suppression of an EMT signature in the cell lines, we focused additional analyses on the expression profiles of primary breast cancer samples, a tumor type in which EMT

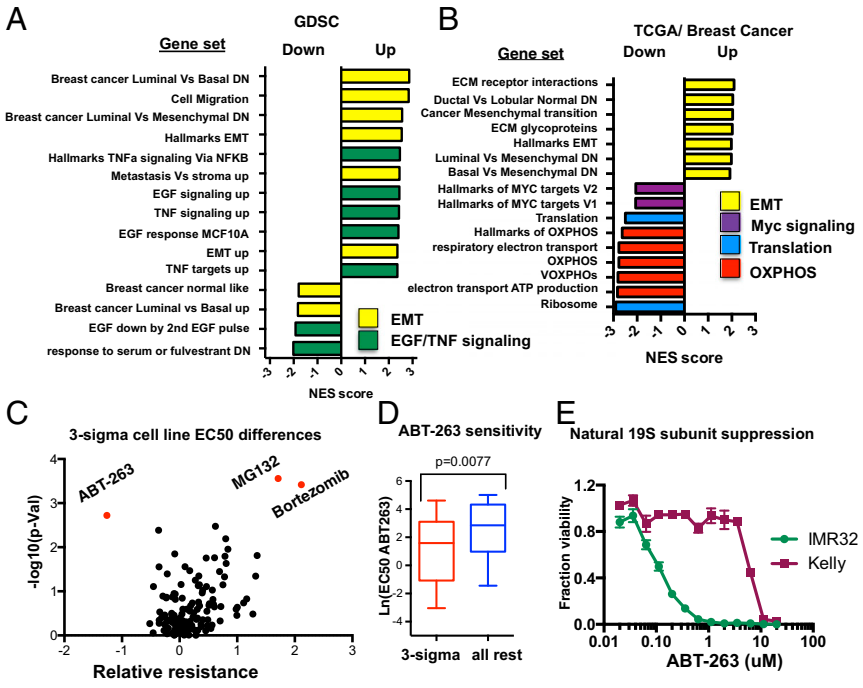

Fig. 3. Proteasome 19S subunit suppression is depictive of a distinct cell state. (*A* and *B*) Gene-set enrichment analysis of genes up- or down-regulated in control but not in the proteasome 3σ cells in the GDSC dataset (*A*) or in primary breast cancer tumors from the TCGA dataset (*B*) (names are abbreviated here but provided in full in Dataset S3). Processes associated with EMT are marked by yellow bars; EGF/TNF-regulated pathways, green bars; Myc signaling, purple bars; mitochondrial oxidative phosphorylation (OXPHOS), red bars; protein translation, blue bars. (*C*) Analysis of drug sensitivity of 3σ and non 3σ groups in the GDSC dataset. The log10 of the *P* values is plotted versus the difference in the log2(EC_{50}) between the 3σ lines and the non 3σ for each drug analyzed. *P* values were calculated by the Student's *t* test. (*D*) The Mann–Whitney test was used to calculate a *P* value for ABT-263 average sensitivity comparing the 3σ and the non 3σ cells in the GDSC dataset. (*E*) Relative viability was examined in IMR32 (natural suppression of PSMD5) and Kelly cells 72 h after addition of the indicated concentrations of ABT-263.

plays a critical role in tumor progression, in invasion, and, ultimately, in systemic metastasis (24, 25). We used mRNA expression data from the TCGA and defined breast tumors as a "control" unless they had a 3σ reduction of at least one subunit of the 19S proteasome. The genes that were specifically enriched in the proteasome 3σ tumors were primarily related to mitochondrial oxidative phosphorylation and to ribosomal biogenesis (Fig. 3*B*, red, and Fig. S3*D*). Such findings suggest that the 3σ tumors might have undergone a less complete shift to aerobic glycolysis ("Warburg effect") and therefore may have retained higher dependency on mitochondrial respiration than the control tumors.

Gene-set enrichment analysis further revealed that the unique signature of the 3σ cancers is conserved between cancer cell lines and primary tumors. For example, the EMT gene signature was largely suppressed in 3σ primary breast tumors (Fig. S3*D*). Extracellular matrix (ECM) genes were also suppressed in the 3σ tumors; ECM genes are highly relevant to both EMT and EGF signaling. Thus, in both established tumor cell lines and in primary tumors, cells with a 3σ reduction in any one 19S proteasome subunit are similar in many other malignancy-related biological pathways.

Naturally Occurring 19S Subunit Suppression Confers Vulnerability to ABT-263. Our data indicate that single-subunit imbalances in the 19S regulatory complex are part of a broad shift in the status of many cancer cells. Using publicly available drug-screening datasets, we asked if this naturally occurring, altered state might change the sensitivity of diverse cancer lines to drugs in addition to proteasome inhibitors. We examined sensitivity data for 140 drugs, most of which were screened against 655 cell lines from the GDSC dataset. For each drug, we calculated the average EC_{50} for all cells in the 3σ group and compared that value to the average EC_{50} for the control group (Fig. 3*C*). As described earlier (Fig. 2), 3σ cell lines were relatively resistant to the proteasome inhibitors MG132 and bortezomib (Fig. 3*C*). The naturally occurring 3σ cell lines, however, were much more sensitive to the BCL2 family inhibitor, ABT-263 (Fig. 4 *C* and *D*; $P = 0.0077$). Analysis of expression levels of BCL2-family genes in the GDSC dataset revealed that the 3σ group had a modestly (but significantly) higher level of expression of BCL2 compared with the control group (Fig. S3*E*). Whether there is a direct mechanistic link between increased expression of BCL2 and inhibitor resistance in cells with suppressed 19S subunits remains to be determined.

We validated the increased vulnerability of 3σ cell lines to ABT-263 in the paired neuroblastoma lines described earlier (Fig. 2*D*). IMR32 cells, in which *PSMD5* is suppressed, were 50- to 100-fold more sensitive to ABT-263 than Kelly cells, which have no subunit suppression (Fig. 3*E*). ABT-263 targets several members of the BCL2 family, including BCL2 and BCL-XL. However, increased sensitivity to proapoptotic drugs was restricted to ABT-263. IMR32 cells did not show enhanced sensitivity to more specific BCL2 (ABT-199), BCL-XL (WEHI 539), and MCL1 (A-1210477) inhibitors (Fig. S3*F*). This finding suggests that, for reasons yet to be defined, the sensitivity of proteasome 3σ cells to ABT-263 is likely due to dual targeting of BCL2 and BCL-XL. As expected, IMR32 cells could be resensitized to a proteasome inhibitor by forced transgenic expression of the PSMD5 subunit (Fig. S3*G*). However, this did not alter their sensitivity to ABT-263 or to the other BCL2 family members, indicating that increased sensitivity to ABT-263 observed in the 19S proteasome 3σ cells was due to an altered cellular state and was not necessarily driven by proteasome subunit unit loss directly.

Mechanisms That Reduce Expression of Specific 19S Proteasome Subunits in Cancers. Rewiring of the transcriptome can result from either genomic aberrations or epigenomic changes. Many chromosomal regions are recurrently lost in cancers, and some of these regions harbor genes that encode 19S proteasome subunits, such as *PSMC2* (26). DNA sequencing data from the CCLE resource enabled us to determine whether the differential reduction in 19S subunit mRNA expression was associated with copy-number loss. Notably, in the majority of 3σ cell lines, the reduced mRNA expression of 19S subunits was not associated with gene-copy-number losses (Fig. 4*A*). For example, in the cases of PSMC3, PSMC4, PSMD3, PSMD5, PSMD7, PSMD8, and PSMD10 subunits, the 3σ lines did not exhibit any copy-number losses involving these genes. Other 19S subunit 3σ lines exhibited partial gene-copy-number losses (Fig. 4*A*). Thus, a mechanism other than gene-copy-number alterations is largely responsible for the reduction of 19S subunit expression in most cancer cell lines.

To investigate further, we examined regulation of *PSMD5* as it was the most frequently suppressed 19S subunit across cancer cell lines and tumors (Fig. 1). A common mechanism suppressing the expression of genes is methylation of their promoters. We assessed PSMD5 promoter methylation in both low-grade gliomas

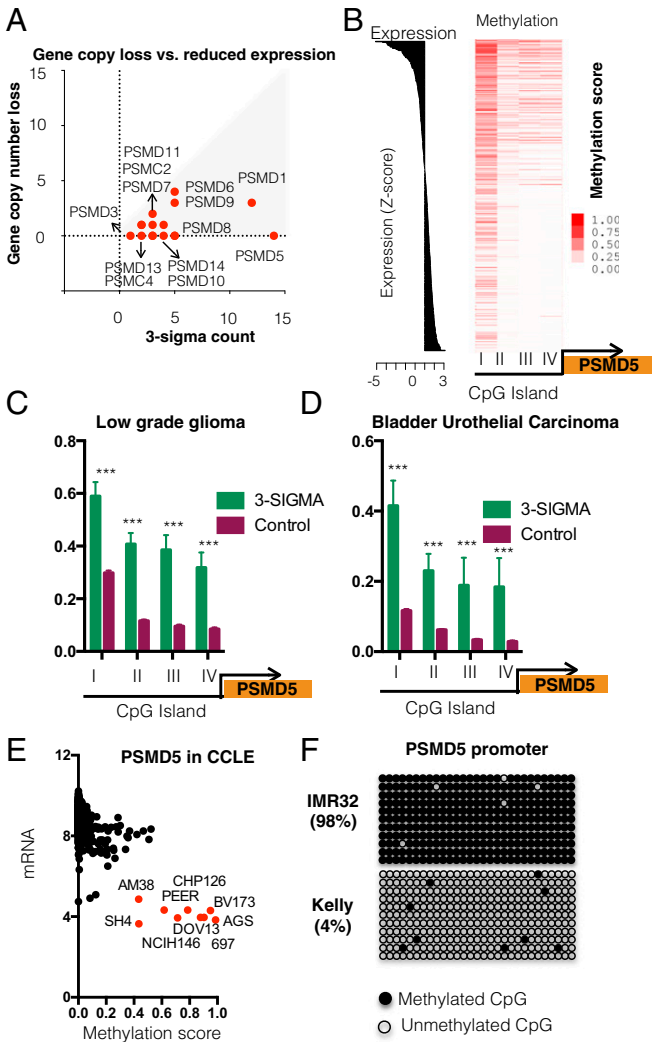

Fig. 4. Suppression of the 19S subunit PSMD5 in a variety of cancers is an epigenetic process regulated by DNA promoter methylation. (*A*) The number of 3σ events versus the number of gene copy loss for every 19S subunit. A cell line was considered to have a copy-number loss if the estimated hybridization was 0.5× the baseline hybridization. (*B*) TCGA dataset analysis for PSMD5 promoter methylation in LGG primary tumors. The data are aligned according to expression levels of the PSMD5 gene (on the left). The methylation score was analyzed for probes I–IV corresponding to genomic coordinates 123605229, 123605234, 123605306, and 123605570, respectively. (*C* and *D*) The average methylation score was calculated for the PSMD5 promoter region in LGG (*C*) and BLCA (*D*) primary tumors. Scores were calculated separately for tumors with a sigma score >3 for the PSMD5 gene (3σ) and the remainder (control). The mean and SEM for every indicated probe is plotted according to the corresponding genomic coordinates. The methylation score was analyzed for probes I–IV corresponding to the same genomic coordinates as in *B*. ***$P <$ 1e-5 (*t* test). (*E*) The mRNA levels and the methylation score for each cell line from the CCLE dataset are plotted for the PSMD5 gene. Annotated cell lines that have reduced expression and a methylated PSMD5 promoter are marked in red. (*F*) The frequency of methylated CpGs in the promoter region of the PSMD5 gene in IMR32 and Kelly cells.

(LGG) and bladder carcinomas (BLCA), tumor types with the highest frequency of PSMD5 3σ samples. In both tumor types, the 19S proteasome 3σ tumors revealed significantly higher methylation of the *PSMD5* promoter (Fig. 4 *B–D* and Fig. S4*A*), suggesting that promoter methylation is a major mechanism for repressing *PSMD5* mRNA expression in cancers.

We next examined the effect of promoter methylation on *PSMD5* gene expression in the CCLE dataset (Fig. 4*E*). Consistent with the results above, suppression of *PSMD5* mRNA expression across different cell lines was strongly correlated with a high methylation score for the promoter region of *PSMD5* (Fig. 4*E*).

To experimentally validate our findings, we returned to our neuroblastoma cell-line pair, IMR32 and Kelly. Confirming CCLE data, our quantitative RT-PCR measurements demonstrated that the relative mRNA expression of all of the 19S subunits was remarkably similar between the two cell lines with the exception of slightly increased levels of *PSMC2* mRNA in the Kelly cells and the expected eightfold decrease in *PSMD5* mRNA in IMR32 cells (Fig. S4*B*). Using DNA bisulfite conversion and sequencing of the *PSMD5* promoter, we found strong DNA methylation of this promoter in IMR32 cells with 98% of the cytosine residues within promoter CpG islands being modified. In contrast, there was minimal methylation of the *PSMD5* promoter in Kelly cells, with only 4% of the cytosines within the CpG islands harboring methyl groups (Fig. 4*F*).

Striking as these findings may be, *PSMD5* was the only 19S proteasome subunit gene showing a strong correlation between suppressed expression and promoter DNA methylation in the CCLE dataset. We therefore suggest that there are multiple pathways by which the suppression of other 19S subunits is achieved. These likely include both genetic and epigenetic mechanisms that, because of their clear relevance to tumor biology, will be important areas of future study.

Discussion

The transcriptional program that regulates proteasome subunit mRNA expression is highly coordinated to maintain the stoichiometric balance of the multiple proteasome components and to foster the efficient assembly of the 26S proteasome complex (27–29). However, a significant change in proteasome complex assembly can result as a consequence of alterations in the level of expression of just a single subunit (26, 30–33). Examining thousands of cancer lines, we show that imbalanced expression of the subunits composing the 19S regulatory complex occurs through a variety of mechanisms. In the case of the PSMD5 subunit, multiple cancers displayed suppression mediated by promoter DNA methylation. However, other subunits did not use this mechanism. Indeed, other laboratories have shown that several types of cancer display chromosomal loss of regions encompassing the locus encoding the *PSMC2* subunit. This deletion has a twofold effect: a decrease both in overall 26S proteasome levels and in the ratio of 26S-to-20S proteasomes (26). Moreover, reduced expression of PSMC2 has been associated with poor response of multiple myeloma patients to carfilzomib treatment (18). Thus, alterations in both DNA methylation and gene copy number are clearly involved in regulating the expression of 19S subunits in a wide variety of cancers. Additional mechanisms, including histone modifications, new mutations, and microRNAs, are also likely to be deployed.

Regardless of the mechanism of suppression, however, the reduction in any one of the many subunits composing the 19S complex reflects a largely altered cellular state characterized by increased resistance to proteasome inhibitors, altered gene-expression signatures, and increased sensitivity to the BCL2 family inhibitor ABT-263 and a small cohort of other clinically relevant drugs. For example, the TNF-NFκB pathway is suppressed in cells that exhibit reduced expression of at least one 19S proteasome subunit. This down-regulation is consistent with the observation that proteasome inhibitors have a strong inhibitory effect on NFκB activation (34). Furthermore, the TNF→NF-κB pathway regulates the transcription of specific proteasome subunits (including *PSMD5*) (35). Perhaps the most striking difference observed in the 3σ group, however, is the altered expression of genes that are associated with the process of EMT. Cell lines in which expression of a single 19S subunit is suppressed display increased epithelial characteristics indicative of a less invasive, less mesenchymal state. Strikingly, in *KRAS* mutant cell lines an enhanced epithelial gene signature correlates with increased sensitivity to ABT-263 (36),

consistent with our findings here. Moreover, analysis of primary breast cancers revealed that 3σ tumors display reduced aerobic glycolysis and higher dependency on oxidative phosphorylation/mitochondrial respiration. At a functional level, it is tempting to speculate that the hypersensitivity to ABT-263, which we find associated with imbalanced 19S subunit expression, is somehow linked to the alterations in mitochondrial physiology suggested by our gene-set enrichment analysis.

Our findings imply that some tumors—or, perhaps equally important, some cancer cells within a heterogeneous tumor—exist in an altered cellular state in which 19S subunit expression is imbalanced. This state appears to be part of a larger cell program that extends beyond the regulation of proteasome function and includes metabolism and signaling. Furthermore, although the more epithelial, more differentiated state marked by regulatory subunit imbalance may be disfavored in the sole context of increased proliferation, it could well serve as a bet-hedging mechanism within the overall tumor to enhance the survival of cells in which protein homeostasis is particularly challenged. Devising orthogonal strategies for targeting this and the other varied epigenetic and phenotypic states available to tumor cells over the course of malignant progression may serve to limit adaptations to chemotherapeutics, block the emergence of drug-resistant clones, and increase our ability to eradicate advanced cancers.

Materials and Methods

Dataset Analysis. Gene expression and drug sensitivity data were downloaded from www.cancerrxgene.org/ (GDSC), https://www.broadinstitute.org/ (CCLE), and https://cancergenome.nih.gov/ (TCGA). For each proteasome subunit gene, a z-score was calculated for each cell line and that was used to plot the expression of individual subunits across all cells in the dataset (see *SI Materials and Methods* for details).

EC50s for the the different drugs were extracted from the GDSC dataset and analyzed as described (see *SI Materials and Methods* for details). Gene copy estimates were extracted and calculated from the CCLE dataset. PSMD5 promoter methylation scores were extracted from both the CCLE and TCGA datasets (see *SI Materials and Methods* for details).

Analysis of expression profiles from the Gene Expression Omnibus (GEO) (https://www.ncbi.nlm.nih.gov/geo/; accession no. GSE51371) (21) were downloaded for the bortezomib-sensitive and -resistant cell-line–derived tumors, and the change in expression of proteasome subunits was calculated (see *SI Materials and Methods* for details).

Pretreatment gene-expression data from relapsed multiple myeloma patients undergoing clinical trials with bortezomib were downloaded from GEO (accession no. GSE51371) (22). Gene-expression data were RMA (robust microarray analysis)-normalized and log-transformed. Sigma scores were calculated from all probes. Patients were binned into two groups: those that had a subunit drop more than 2.8 sigma and those that did not. For each group, the time to relapse from bortezomib treatment was plotted as a Kaplan–Meier plot. *P* value was calculated using the Wilcoxon test.

Cell Culture Methods. Kelly, IMR32, OVCAR3, and OVSAHO were cultured in RPMI-1640 (OVCAR3 was supplemented with 0.01 mg/mL insulin) medium supplemented with 10% FBS.

DNA Methylation Sequencing. DNA was extracted from IMR32 and Kelly cells with a DNeasy Blood and Tissue Kit (Qiagen) according to the manufacturer's protocol. Bisulfate conversion of the DNA was conducted using the EpiTect Bisulfite Kit (Qiagen) according to the manufacturer's protocol. The modified DNA was then used as a template for PCR of the PSMD5 promoter (see *SI Materials and Methods* for details).

ACKNOWLEDGMENTS. We thank Brad Bernstein, Anthony Letai, Jeremy Ryan, Yonatan Stelzer, Linda Clayton, Marc Mendillo, and Ruthie Scherz-Shouval for helpful discussion and comments. P. Tsvetkov was supported by EMBO Fellowship ALTF 739-2011 and by the Charles A. King Trust Postdoctoral Fellowship Program. S.L. was an investigator of the Howard Hughes Medical Institute.

1. Varshavsky A (2012) Three decades of studies to understand the functions of the ubiquitin family. *Methods Mol Biol* 832:1–11.
2. Deshaies RJ (2014) Proteotoxic crisis, the ubiquitin-proteasome system, and cancer therapy. *BMC Biol* 12:94.
3. Labbadia J, Morimoto RI (2015) The biology of proteostasis in aging and disease. *Annu Rev Biochem* 84:435–464.
4. Mendillo ML, et al. (2012) HSF1 drives a transcriptional program distinct from heat shock to support highly malignant human cancers. *Cell* 150(3):549–562.
5. Adams J, Palombella VJ, Elliott PJ (2000) Proteasome inhibition: A new strategy in cancer treatment. *Invest New Drugs* 18(2):109–121.
6. Kumar MS, et al. (2012) The GATA2 transcriptional network is requisite for RAS oncogene-driven non-small cell lung cancer. *Cell* 149(3):642–655.
7. Luo J, et al. (2009) A genome-wide RNAi screen identifies multiple synthetic lethal interactions with the Ras oncogene. *Cell* 137(5):835–848.
8. Petrocca F, et al. (2013) A genome-wide siRNA screen identifies proteasome addiction as a vulnerability of basal-like triple-negative breast cancer cells. *Cancer Cell* 24(2):182–196.
9. Chen D, Frezza M, Schmitt S, Kanwar J, Dou QP (2011) Bortezomib as the first proteasome inhibitor anticancer drug: Current status and future perspectives. *Curr Cancer Drug Targets* 11(3):239–253.
10. Crawford LJ, Irvine AE (2013) Targeting the ubiquitin proteasome system in haematological malignancies. *Blood Rev* 27(6):297–304.
11. Kale AJ, Moore BS (2012) Molecular mechanisms of acquired proteasome inhibitor resistance. *J Med Chem* 55(23):10317–10327.
12. Suzuki E, et al. (2011) Molecular mechanisms of bortezomib resistant adenocarcinoma cells. *PLoS One* 6(12):e27996.
13. Lichter DI, et al. (2012) Sequence analysis of β-subunit genes of the 20S proteasome in patients with relapsed multiple myeloma treated with bortezomib or dexamethasone. *Blood* 120(23):4513–4516.
14. Markovina S, et al. (2008) Bortezomib-resistant nuclear factor-kappaB activity in multiple myeloma cells. *Mol Cancer Res* 6(8):1356–1364.
15. Li B, et al. (2015) The nuclear factor (erythroid-derived 2)-like 2 and proteasome maturation protein axis mediate bortezomib resistance in multiple myeloma. *J Biol Chem* 290(50):29854–29868.
16. Shringarpure R, et al. (2006) Gene expression analysis of B-lymphoma cells resistant and sensitive to bortezomib. *Br J Haematol* 134(2):145–156.
17. Zhang XD, et al. (2016) Tight junction protein 1 modulates proteasome capacity and proteasome inhibitor sensitivity in multiple myeloma via EGFR/JAK1/STAT3 signaling. *Cancer Cell* 29(5):639–652.
18. Acosta-Alvear D, et al. (2015) Paradoxical resistance of multiple myeloma to proteasome inhibitors by decreased levels of 19S proteasomal subunits. *eLife* 4:e08153.
19. Tsvetkov P, et al. (2015) Compromising the 19S proteasome complex protects cells from reduced flux through the proteasome. *eLife* 4:4.
20. Garnett MJ, et al. (2012) Systematic identification of genomic markers of drug sensitivity in cancer cells. *Nature* 483(7391):570–575.
21. Moros A, et al. (2014) Synergistic antitumor activity of lenalidomide with the BET bromodomain inhibitor CPI203 in bortezomib-resistant mantle cell lymphoma. *Leukemia* 28(10):2049–2059.
22. Mulligan G, et al. (2007) Gene expression profiling and correlation with outcome in clinical trials of the proteasome inhibitor bortezomib. *Blood* 109(8):3177–3188.
23. Roué G, et al. (2011) The Hsp90 inhibitor IPI-504 overcomes bortezomib resistance in mantle cell lymphoma in vitro and in vivo by down-regulation of the prosurvival ER chaperone BiP/Grp78. *Blood* 117(4):1270–1279.
24. Kalluri R, Weinberg RA (2009) The basics of epithelial-mesenchymal transition. *J Clin Invest* 119(6):1420–1428.
25. Mani SA, et al. (2008) The epithelial-mesenchymal transition generates cells with properties of stem cells. *Cell* 133(4):704–715.
26. Nijhawan D, et al. (2012) Cancer vulnerabilities unveiled by genomic loss. *Cell* 150(4):842–854.
27. Radhakrishnan SK, et al. (2010) Transcription factor Nrf1 mediates the proteasome recovery pathway after proteasome inhibition in mammalian cells. *Mol Cell* 38(1):17–28.
28. Sha Z, Goldberg AL (2014) Proteasome-mediated processing of Nrf1 is essential for coordinate induction of all proteasome subunits and p97. *Curr Biol* 24(14):1573–1583.
29. Xie Y, Varshavsky A (2001) RPN4 is a ligand, substrate, and transcriptional regulator of the 26S proteasome: A negative feedback circuit. *Proc Natl Acad Sci USA* 98(6):3056–3061.
30. Lokireddy S, Kukushkin NV, Goldberg AL (2015) cAMP-induced phosphorylation of 26S proteasomes on Rpn6/PSMD11 enhances their activity and the degradation of misfolded proteins. *Proc Natl Acad Sci USA* 112(52):E7176–E7185.
31. Rousseau A, Bertolotti A (2016) An evolutionarily conserved pathway controls proteasome homeostasis. *Nature* 536(7615):184–189.
32. Vilchez D, et al. (2012) Increased proteasome activity in human embryonic stem cells is regulated by PSMD11. *Nature* 489(7415):304–308.
33. Vilchez D, et al. (2012) RPN-6 determines C. elegans longevity under proteotoxic stress conditions. *Nature* 489(7415):263–268.
34. Sunwoo JB, et al. (2001) Novel proteasome inhibitor PS-341 inhibits activation of nuclear factor-kappa B, cell survival, tumor growth, and angiogenesis in squamous cell carcinoma. *Clin Cancer Res* 7(5):1419–1428.
35. Shim SM, et al. (2012) Role of S5b/PSMD5 in proteasome inhibition caused by TNF-α/NFκB in higher eukaryotes. *Cell Reports* 2(3):603–615.
36. Corcoran RB, et al. (2013) Synthetic lethal interaction of combined BCL-XL and MEK inhibition promotes tumor regressions in KRAS mutant cancer models. *Cancer Cell* 23(1):121–128.